

DYNAMICS OF THE FUNDAMENTAL MATTER-WAVE SOLITONS IN A TIME-MODULATED TWO-DIMENSIONAL QUASIPERIODIC OPTICAL LATTICE.

SALOMÓN GARCÍA-PAREDES*

Centro de Investigación en Ingeniería y Ciencias Aplicadas
Universidad Autónoma del Estado de Morelos,
Cuernavaca, Mor. 62209, México

GENNADIY BURLAK†

Centro de Investigación en Ingeniería y Ciencias Aplicadas
Universidad Autónoma del Estado de Morelos,
Cuernavaca, Mor. 62209, México

(Communicated by Vladimir Rabinovich)

Abstract

By means of the variational approximation (VA) and systematic simulations, we study dynamics and stability boundaries for fundamental solitons in a two-dimensional (2D) self-attracting Bose-Einstein condensate (BEC), trapped in an quasiperiodic optical lattice (OL), with the amplitude subject to periodic time modulation (the modulation frequency, ω). Regions of stability of the solitons against the collapse and decay are identified in the space of the model's parameters.

AMS Subject Classification: 35C08; 37K40; 35J10; 35J66.

Keywords: Bose-Einstein condensate, fundamental solitons, quasiperiodic optical lattice, numerical simulations.

1 INTRODUCTION

Nowadays, solitons have an important role in physics and mathematics. Also, they have reached other disciplines such as biology, genomic, optics, astronomy, i.e. One of the most important studies in solitons has been the study of their different dynamics [1], in particular those which relate to the two-dimensional (2D). In the last 15 years a challenging subject

*E-mail address: salomon.garcia@uaem.mx

†E-mail address: gburlak@uaem.mx

in the study of dynamic patterns in Bose-Einstein condensates (BECs) is the investigation of matter-wave solitons in multidimensional settings [2].

Our aim in this paper is to demonstrate the stability in different families of solitons, showing the ranges (frequency, amplitude, optical potential and time) in which the solitons are stable, using a full OL.

It is proved, that the existence of stability in solitons 2D is mainly due to the existence and management techniques of optical lattices (OL) [3] in time-periodic modulation, however, this stability could be destroyed, causing a collapse.

In our study, we use the two dimensional Gross-Pitaevskii equation (GPE) for mean-field wave function $\Psi(x, y, t)$ with time-modulated OL [2]

$$i \frac{\partial \Psi}{\partial t} = -\frac{1}{2} \left(\frac{\partial^2}{\partial x^2} + \frac{\partial^2}{\partial y^2} \right) \Psi - g_0 |\Psi|^2 \Psi - V_0 \left[1 + \frac{\varepsilon}{2} \cos(\omega t) \right] V(x, y) \Psi, \quad (1.1)$$

where ω is the frequency, ε is the amplitude, V_0 is the optical potential, t is the time and (x, y) are coordinates in 2D of the OL. At $g = 1$ the nonlinearity is attractive. Here the quasiperiodic (QP) lattice potential of depth $2V_0$ is taken as [3, 4, 5]

$$V(x, y) = -V_0 \sum_{n=1}^M \cos(\mathbf{k}^{(n)} \mathbf{r}), \quad (1.2)$$

with the set of wave vectors $\mathbf{k}^{(n)} = k\{\cos(2\pi(n-1)/M), \sin(2\pi(n-1)/M)\}$ and $M = 5$ or $M \geq 7$. Here, following Ref. [4], we focus on the basic case of the Penrose-tiling potential, corresponding to $M = 5$. The 2D profile of such QP potential is displayed below in Fig. 1.

Setting $V_0 > 0$, the center of the 2D soliton will be placed at the local minimum of the potential (2), $x = y = 0$. The solitons will be characterized by the norm, defined as usual: $N = \int \int |\Psi(x, y)|^2 dx dy$. The quantity N relates to the actual number of atoms in the condensate, \mathcal{N} , by means of standard rescaling [6]: $\mathcal{N} = (a_\perp / 4\pi a_s) N$, where a_\perp (typically, $\sim \mu\text{m}$) and a_s ($\sim 0.1 \text{ nm}$) are the transverse trapping length of the condensate and scattering length of the atomic collisions, respectively. In optics, the same equation (1.1), with t replaced by the propagation distance, z , governs the transmission of electromagnetic waves with local amplitude Ψ in the bulk waveguide with the transverse QP modulation of the refractive index. In the latter case, N is proportional to the beam's total power.

Numerical results: soliton families. Simulations of Eq. (1.1) are performed on the 2D numerical grid of size 128×128 , starting with the input in the form of an isotropic Gaussian,

$$\Psi(x, y) = A_0 \exp(-q(x^2 + y^2)). \quad (1.3)$$

Initial amplitude A_0 , along with the OL depth and wavenumber, V_0 and k , were varied, while the initial width was fixed by setting $q = 0.9$ [which is possible by means of rescaling of Eq. (1.1)].

Before proceeding to numerical results, it is worth to note that, although the application of the variational approximation, which is a ubiquitous analytical tool for the study of bound states in nonlinear systems [7][8], to 2D solitons in QP potentials is possible [3], the simplest isotropic *ansatz*, taken in the same form as Gaussian (1.3), cannot capture peculiarities of the setting based on the QP potential. Indeed, the part of the Lagrangian accounting for the interaction of *ansatz* (1.3) with the underlying OL potential (1.2) consists

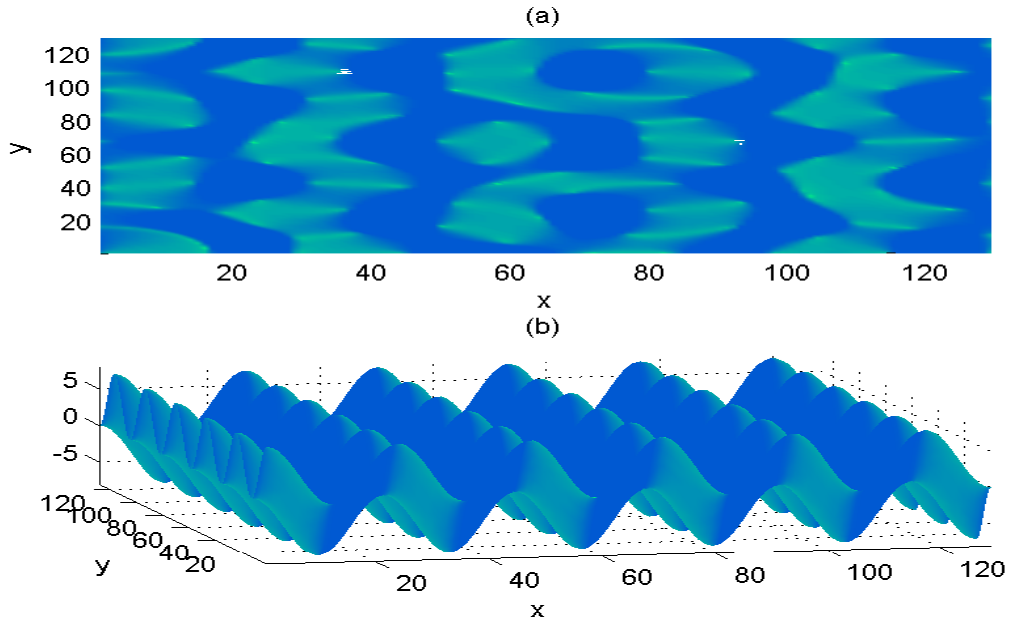


Figure 1. (Color on line.) Examples of optical lattices. a) Quasiperiodic OL. b) Periodic OL.

of integrals like $V_0 A_0^2 \int \int \cos(\mathbf{k}^{(n)} \mathbf{r}) \exp(-2qr^2) d\mathbf{r} = \pi [V_0/(2q)] \exp[-k^2/(8q)]$. Being insensitive to the particular orientation of wave vectors $\mathbf{k}^{(n)}$, this approximation is too coarse. It may be improved by using an anisotropic ansatz, but it will render the variational analysis cumbersome.

The first objective is to construct families of localized ground-state modes, in the form of $\Psi(x, y, t) = \exp(-i\mu t)\varphi(x, y)$, with real wave function $\varphi(x, y)$ found by means of the accelerated imaginary-time method [9]. Following the convention commonly adopted in physics literature [3][7][8][10][11][12], we refer to these modes as “solitons”, even though they do not feature the unhindered motion characteristic to “genuine” solitons. The simulations of Eq. (1.1), rewritten in the imaginary time with a fixed value of μ , quickly converge to the ground state, with $\lesssim 1000$ iterations necessary to reduce the residual error to the level of 10^{-10} .

2 THE VARIATIONAL APPROXIMATION.

Variational methods have been quite useful in many problems of nonlinear optics and BEC. To apply the VA to the present model, we notice that Eq. (1.1) can be derived from Lagrangian $L = \int_{-\infty}^{+\infty} \mathcal{L} dx dy$, with density

$$\mathcal{L} = \frac{i}{2} (\Psi^* \Psi_t - \Psi \Psi_t^*) - \frac{1}{2} (|\Psi_x|^2 + |\Psi_y|^2) + \frac{1}{2} |\Psi|^4 + V_0(x, y) T(t) |\Psi|^2, \quad (2.1)$$

where the asterisk stands for the complex conjugation. In this paper we adopt the anisotropic *ansatz* for the soliton in the form

$$\Psi_{\text{ans}}(x, y, t) = A(t) \exp\left(i\phi(t) + \frac{i}{2}[b_x(t)x^2 + b_y(t)y^2] - \frac{1}{2}\left[\frac{x^2}{W_x^2(t)} + \frac{y^2}{W_y^2(t)}\right]\right), \quad (2.2)$$

where all variables $A(t)$, $\phi(t)$, $b_{1,2}(t)$, and $W_{1,2}(t)$ (amplitude, phase, radial *chirp*, and radial width, respectively) are real. Tractable, although rather cumbersome, variational equations below are generated by an anisotropic ansatz (2.2), with different widths and chirps along axis x and y . The substitution of the ansatz in Eq. (2.1) and calculation of the integrals yield the effective Lagrangian,

$$L_{\text{eff}} = -N \frac{d\phi}{dt} - \frac{1}{4} W_1^2 N \frac{db_1}{dt} - \frac{1}{4} W_2^2 N \frac{db_2}{dt} - \frac{1}{4} \frac{N}{W_1^2} - \frac{1}{4} \frac{N}{W_2^2} - \frac{1}{4} W_1^2 N b_1^2 - \frac{1}{4} W_2^2 N b_2^2 \quad (2.3)$$

$$+ NV_0 T(t) e^{-W_1^2} + NV_0 T(t) e^{-W_2^2} + \frac{N^2}{4\pi W_2 W_1},$$

where $\pi A^2 W_1(t) W_2(t) = N$ is tantamount to the conservation of the norm of the wave function, $T(t) = 1 + \frac{\varepsilon}{2} \cos(\omega t)$, $b_i = W_i^{-1} (dW_i/dt)$.

For isotropic VA case $W_{1,2} = W$, $b_{1,2} = b$, such Lagrangian is reduced to well-known form [2]

$$L_{\text{eff}} = -N \frac{d\phi}{dt} - \frac{N}{2W^2} + \frac{N^2}{4\pi W^2} + 2V_0 \left[1 + \frac{\varepsilon}{2} \cos(\omega t)\right] N e^{-W^2} - \frac{1}{2} \frac{db}{dt} N W^2 - \frac{1}{2} b^2 N W^2.$$

Using these relations, the next variational equations from Eq.(2.3) can be cast in the following final form,

$$\frac{d^2 W_1}{dt^2} = \frac{1}{W_1^2} \left(\frac{1}{W_1} - \frac{N/\tilde{N}_{\text{max}}}{W_2} \right) - 4V_0 T(t) W_1 \exp(-W_1^2),$$

$$\frac{d^2 W_2}{dt^2} = \frac{1}{W_2^2} \left(\frac{1}{W_2} - \frac{N/\tilde{N}_{\text{max}}}{W_1} \right) - 4V_0 T(t) W_2 \exp(-W_2^2).$$

For isotropic case $W_{1,2} = W$ such system is reduced to one equation[2]

$$\frac{d^2 W}{dt^2} = \frac{1 - N/\tilde{N}_{\text{max}}}{W^3} - 4V_0 \left[1 + \frac{\varepsilon}{2} \cos(\omega t)\right] W \exp(-W^2), \quad (2.4)$$

where $\tilde{N}_{\text{max}} \equiv 2\pi$ is the well-known VA prediction for the critical (maximum) norm in the 2D space, which separates collapsing solutions at $N > \tilde{N}_{\text{max}}$.

3 NUMERICS.

In our simulations it is implemented a two-step procedure: (i) generation the ground state soliton from Eq. (1.3), and then (ii) the study of the dynamics of such solution in the time-modulated OL.

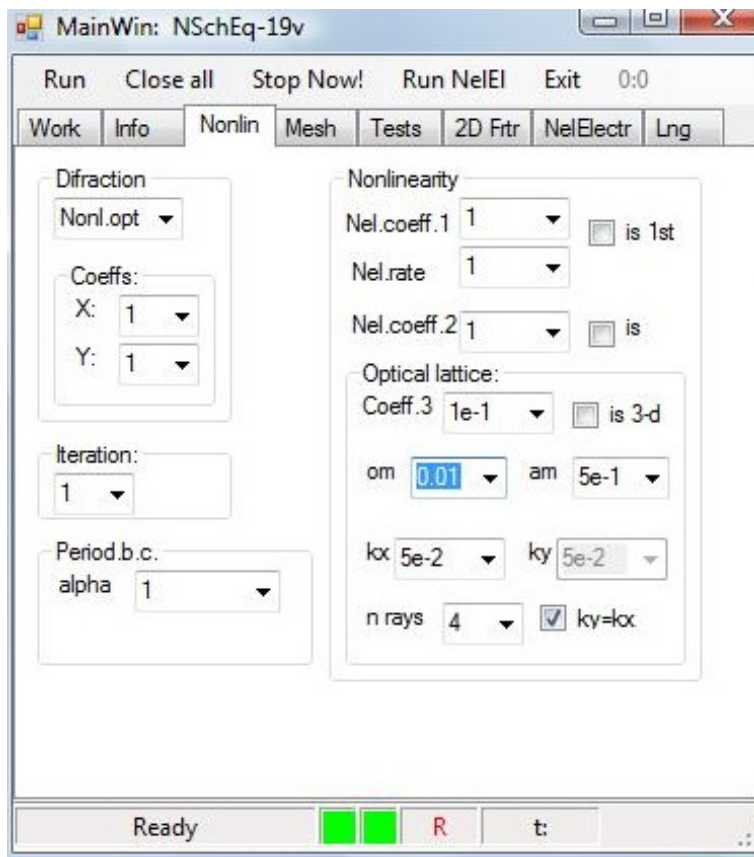


Figure 2. (Color on line.) The graphic user interface (GUI) for the program that is used for our simulations.

The numerical simulations are performed by means of the split-step method [13], [14], with implemented a graphic user interface (GUI) that is shown in Fig. 2)

Fig. 3 shows chemical potential μ of the ground-state solitons versus its norm N , at two fixed wavenumbers of the Penrose-tiling potential, $k = 1$ (a) and $k = 1.5$ (c) and various values of its depth, V_0 [see Eq. (1.2)]. Fig. 5 shows $\mu(N)$ for the fixed depth of the lattice potential, and different values of its wavenumber. Labels C_j and A_j ($j = 1, 2, 3, 4$) indicate VK-stable and unstable branches with $d\mu/dN < 0$ and $d\mu/dN > 0$, respectively. Points B_j mark boundaries between the stable and unstable branches, at which $d\mu/dN = 0$ diverges.

To gain the insight into the behavior of such a system we have to verify if the found ground state contains less number of particles than initial one. Since the imaginary-time algorithm[9] of the ground state calculation does not conserve the number of particles, there rises a question on the relation of number of particles of initial condition N_i (see Eq.(1.3)) to numbers of particles N for resulting ground state. Very conditionally one can say that at $N < N_i$ soliton returns atoms to the bath, while at $N > N_i$ soliton accepts atoms from a bath and thus can be only quasistable one. For systems with a small number of particles (that is supposed in this paper), the latter it is difficult to realize. So that a soliton state with parameters $p(N) = N/N_i > 1$ is at least a quasi-stable one.

As said above, the main point in this work is the determination of the stability of the solitons close to the critical points B_j correspond the junctions of stable and unstable solution families, at which $d\mu/dN = \infty$ in the time varying OL. This was done by means of long-time simulations. Fig. 6 shows the dynamic of stable 2D soliton, where a) frequency $\omega = 0.9$, amplitude $\varepsilon = 0.6$ and the optical potential $V_0 = 2$. b) frequency $\omega = 1.0$, amplitude $\varepsilon = 0.6$ and the optical potential $V_0 = 2$.

An example of collapsed soliton is shown in Fig.7. From Fig.7 we observe that a) If the frequency $\omega < 2.5$, and $\varepsilon = 0.6$, $V_0 = 2$, a soliton is slowly destructed (by collapse or decay), and b) at $\omega = 2.29$, the collapse starts much earlier.

Fig.8 displays: a) Stable soliton where $\omega = 0.02$, amplitude $\varepsilon = 0.5$ and the optical potential $V_0 = 1$. b) frequency $\omega = 1.0$, amplitude $\varepsilon = 0.6$ and the optical potential $V_0 = 1$. b) Stable soliton where $\omega = 0.02$, amplitude $\varepsilon = 0.5$ and the optical potential $V_0 = 1$. b) frequency $\omega = 0.2$, amplitude $\varepsilon = 0.5$ and the optical potential $V_0 = 1$

A typical example of a collapsed soliton is shown in Fig. 9, where a) Collapsed soliton where $\omega = 0.29$, amplitude $\varepsilon = 0.5$ and the optical potential $V_0 = 1$. b) frequency $\omega = 0.35$, amplitude $\varepsilon = 0.5$ and the optical potential $V_0 = 1$.

V_0	n_l	ϵ	ω
1	5	0.5	$0.2 \geq \omega \leq 2.0$
2	5	0.6	$0.2 \geq \omega \leq 3.0$
3	5	0.6	$1.6 \geq \omega \leq 3.0$
2	5	0.8	$0.9 \geq \omega \leq 1.2$

(3.1)

Table 1: Setting the values for V_0 , n_l , and ϵ ,estables solitons can be obtained between the range of ω , as described above.

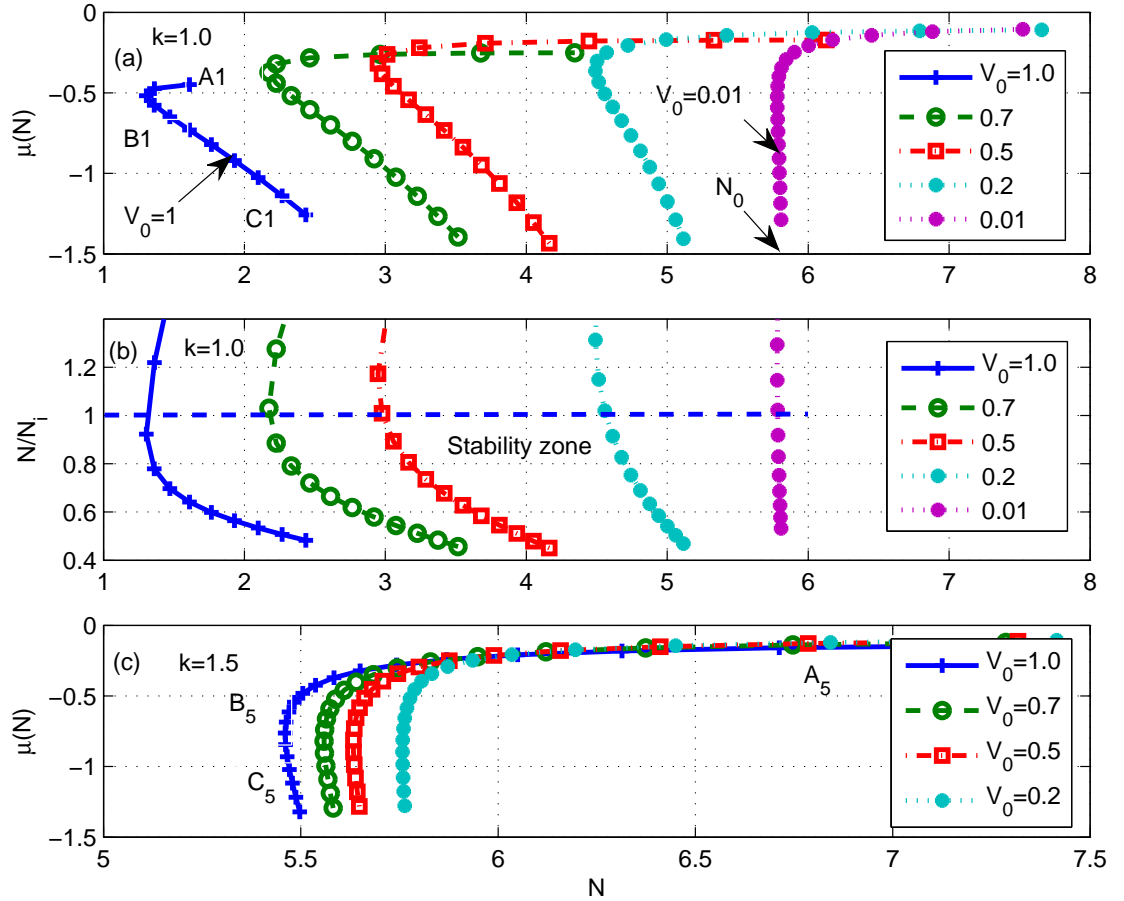


Figure 3. (Color online.) Chemical potential μ of the ground-state solitons versus its norm N , at two fixed wavenumbers of the Penrose-tiling potential, $k = 1$ (a) and $k = 1.5$ (c) and various values of its depth, V_0 [see Eq. (1.2)]. Labels C_j and A_j ($j = 1, 2, 3, 4$) indicate VK-stable and unstable branches with $d\mu/dN < 0$ and $d\mu/dN > 0$, respectively. Points B_j mark boundaries between the stable and unstable branches, at which $d\mu/dN = 0$ diverges. Value $N_0 \approx 5.84$ (for $V_0 = 0.01$) is close to the limit value of N corresponding to the norm of the townes' soliton. Panel (b) shows parameter $p = N/N_i$ for $k = 1.0$. We observe that areas N with $p < 1$ correspond to area where $d\mu/dN < 0$ (stability zone). See details in text.

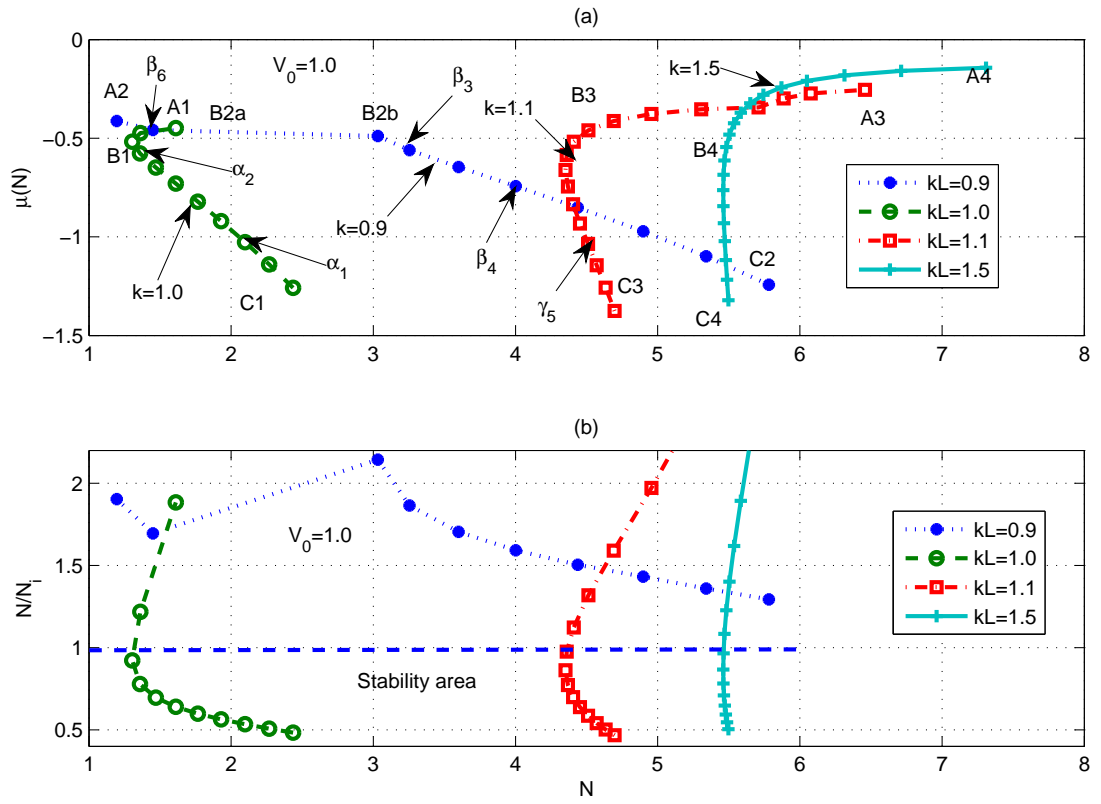


Figure 4. (Color on line.) Fixed depth of the OL and different values of its wavenumber.

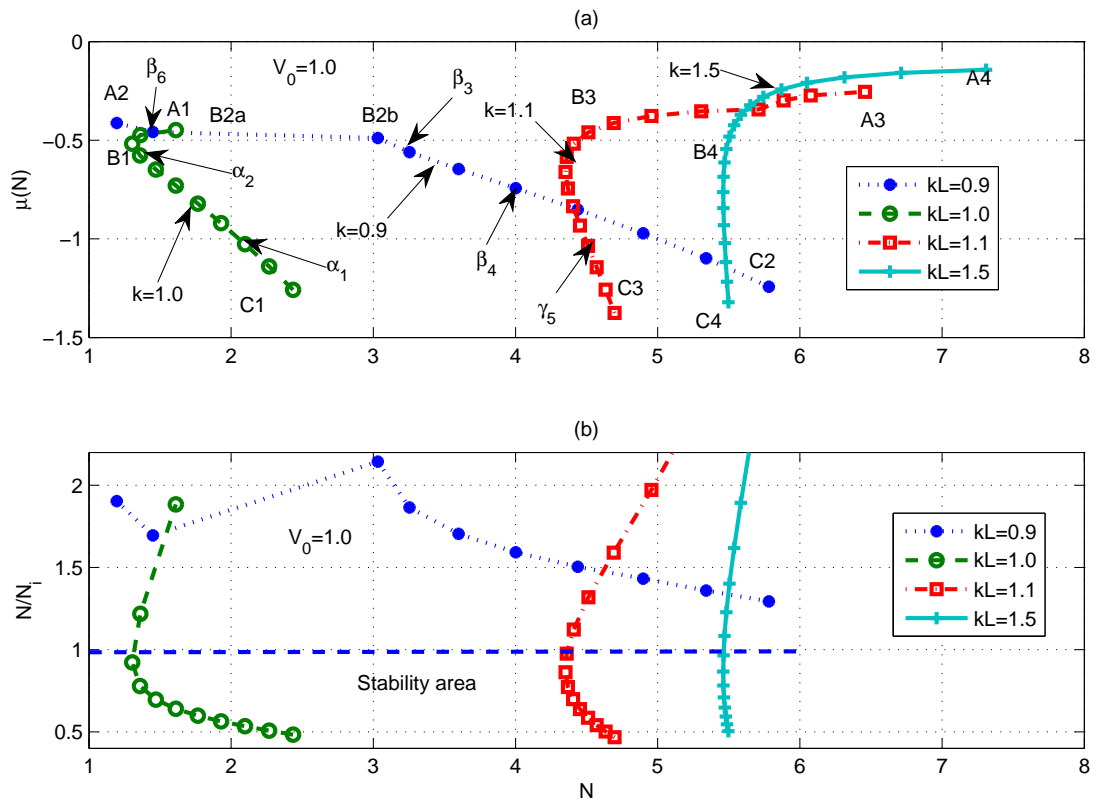


Figure 5. Fixed depth of the OL and different values of its wavenumber.

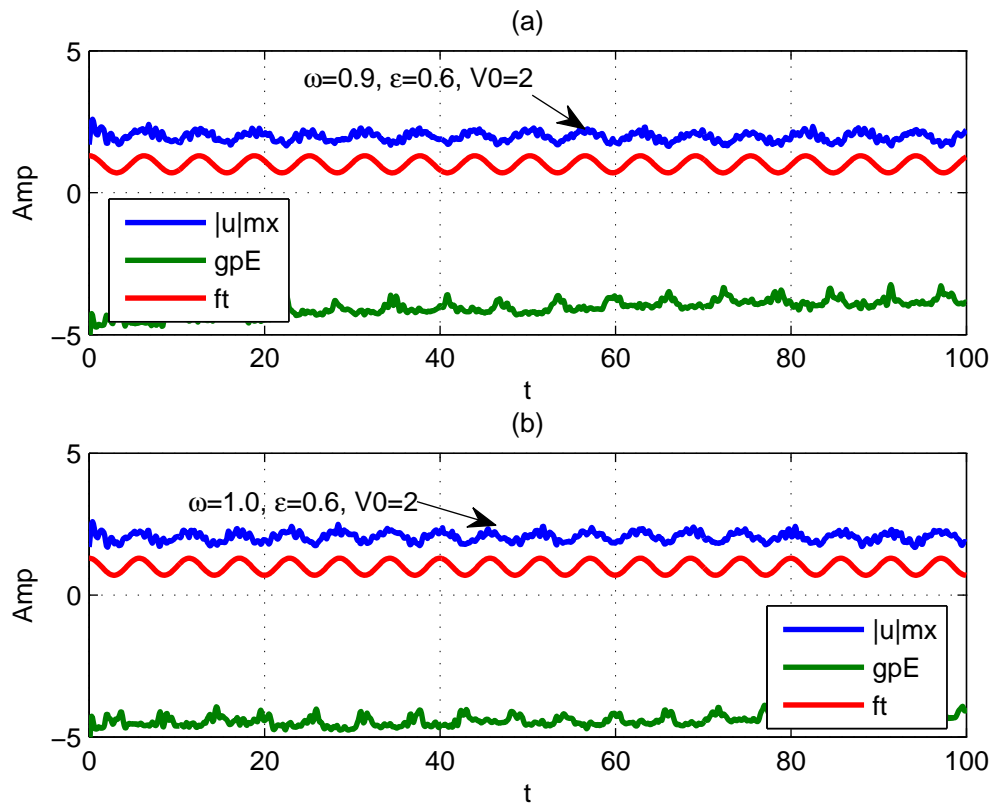


Figure 6. (Color on line.) Dynamic for stable 2D soliton, where a) frequency $\omega = 0.9$, amplitude $\varepsilon = 0.6$ and the optical potential $V_0 = 2$. b) frequency $\omega = 1.0$, amplitude $\varepsilon = 0.6$ and the optical potential $V_0 = 2$

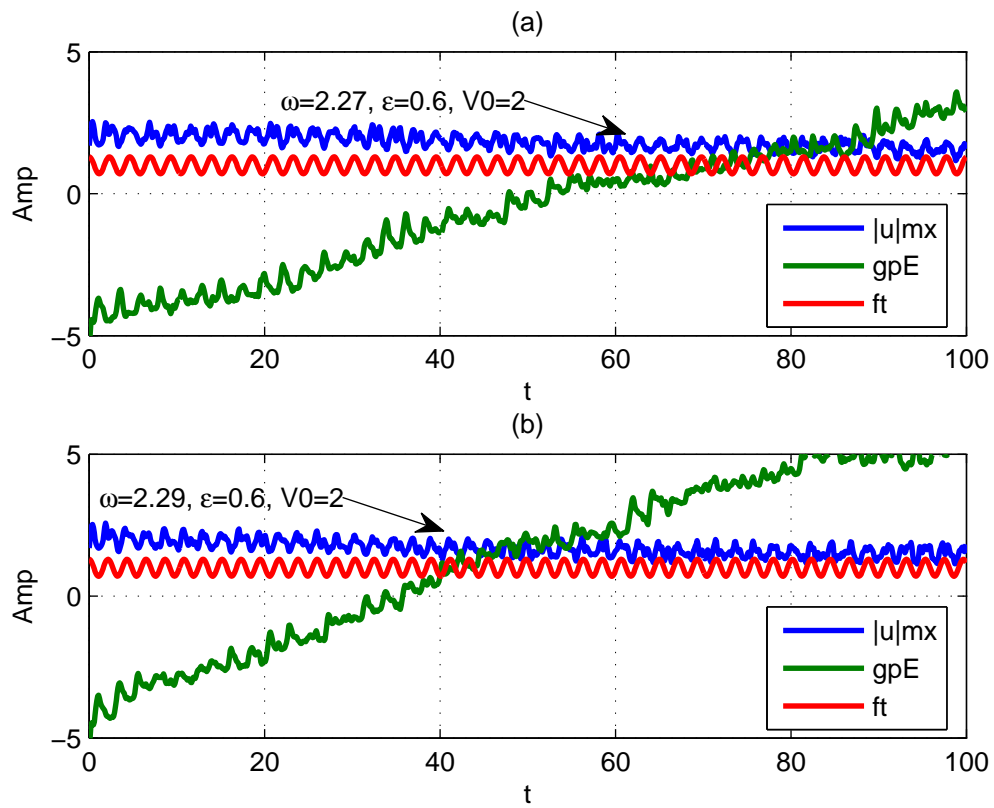


Figure 7. (Color on line.) An example of collapsed soliton. a) If the frequency $\omega < 2.5$, and $\varepsilon = 0.6$, $V_0 = 2$, a collapsed soliton is obtained. b) If $\omega = 2.29$, the collapse will be obtained much faster.

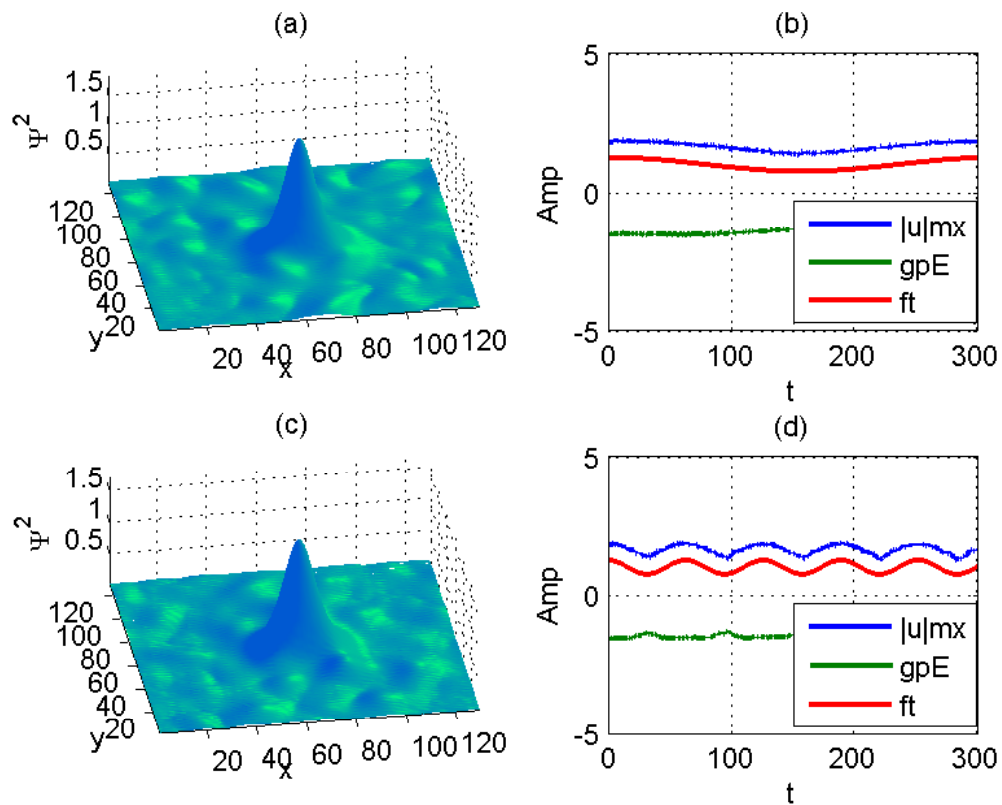


Figure 8. (Color on line.) a) Stable soliton where frequency $\omega = 0.02$, amplitude $\varepsilon = 0.5$ and the optical potential $V_0 = 1$. b) frequency $\omega = 1.0$, amplitude $\varepsilon = 0.6$ and the optical potential $V_0 = 1$. c) frequency $\omega = 0.2$, amplitude $\varepsilon = 0.5$ and the optical potential $V_0 = 1$

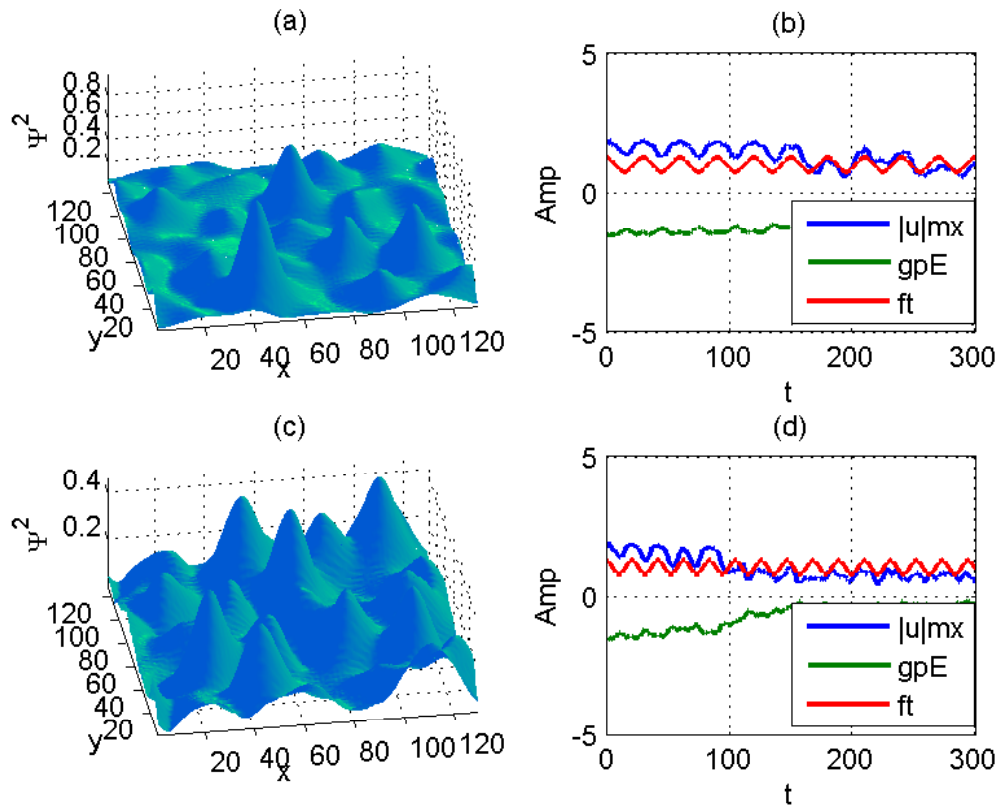


Figure 9. (Color on line.) A typical example of a collapsed soliton. a) Collapsed soliton where $\omega = 0.29$, amplitude $\varepsilon = 0.5$ and the optical potential $V_0 = 1$. b) frequency $\omega = 0.35$, amplitude $\varepsilon = 0.5$ and the optical potential $V_0 = 1$.

4 Conclusions

1. We have studied the dynamics of 2D solitons in the model of trapped BEC OL square (optical lattice) whose strength is subject to modulation in time. Experimental results on the model belongs to a broad class of schemes for the running GUI.

2. Through the VA (variational approximation) is derived here for the advanced asymmetrical (AVA) case we plan to compare the results of AVA with and direct systematic simulations of soliton dynamics in quasiperiodical lattice in our future publications.

5 Acknowledgments

Prof. B. A. Malomed is gratefully acknowledged for useful discussions. This work was partially supported by CONACyT (México) grants No. 169496, No. 168104, and project Redes de PROMEP (México).

References

- [1] B. A. Malomed, *Soliton Management in Periodic Systems*, Springer, New York 2006.
- [2] G. Burlak and B. A. Malomed, Dynamics of matter-wave solitons in a time-modulated two-dimensional optical lattice. *Phys. Rev. A*, **77**, (2008), 053606.
- [3] B. B. Baizakov, B. A. Malomed, and M. Salerno, *Nonlinear Waves: Classical and Quantum Aspects*, Kluwer Academic Publishers, Dordrecht 2004, pp 61-80.
- [4] H. Sakaguchi and B. A. Malomed, Gap solitons in quasiperiodic optical lattices. *Phys. Rev. E* **74** (2006), 026601.
- [5] G. Burlak and A. Klimov, The solitons redistribution in Bose–Einstein condensate in quasiperiodic optical lattice. *Phys. Lett. A*, **369** (2007), pp 510-516.
- [6] F. Dalfovo, S. Giorgini, and L. P. Pitaevskii, Theory of Bose-Einstein condensation in trapped gases. *Rev. Mod. Phys.* **71** (1999), pp 463-486.
- [7] B. A. Malomed, D. Mihalache, F. Wise, and L. Torner, Spatiotemporal optical solitons. *Optics B: Quant. Semics. Opt.* **7** (2005), R53.
- [8] Y. V. Kartashov, B. A. Malomed, and L. Torner, Solitons in nonlinear lattices. *Rev. Mod. Phys.* **83** (2011), pp 247-271.
- [9] J. Yang and T. I. Lakoba, Accelerated imaginary-time evolution methods for the computation of solitary waves. *Stud. Appl. Math.* **120** (2008), pp 265-271.
- [10] F. Lederer, G. I. Stegeman, D. N. Christodoulides, G. Assanto, M. Segev, and Y. Silberberg, Discrete solitons in optics. *Phys. Rep.* **463** (2008), pp 1-55.
- [11] B. B. Baizakov, B. A. Malomed, and M. Salerno, Multidimensional solitons in periodic potentials. *Europhys. Lett.* **63** (2003), pp 642-649.

- [12] B. B. Baizakov, B. A. Malomed, and M. Salerno, Multidimensional solitons in a low-dimensional periodic potential. *Phys. Rev. A*, **70** (2004), 053613.
- [13] J. Yang. *Nonlinear waves in integrable and nonintegrable systems*, SIAM-USA, 2010.
- [14] W. H. Press, S. A. Teukovsky, W. T. Vetterling, and B. P. Flannery, *Numerical recipes in C++*, Cambridge University Press, Cambridge 2002.